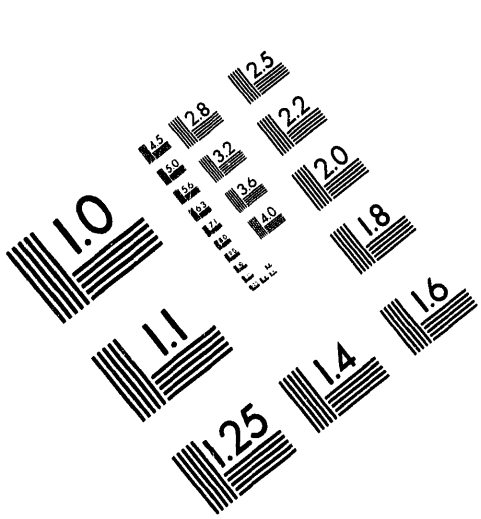

Association for Information and Image Management
1100 Wayne Avenue, Suite 1100
Silver Spring, Maryland 20910
301/587-8202

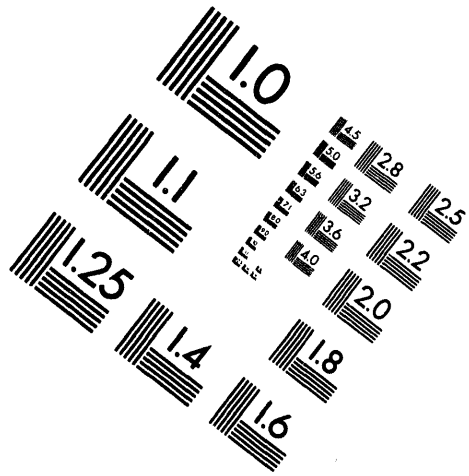

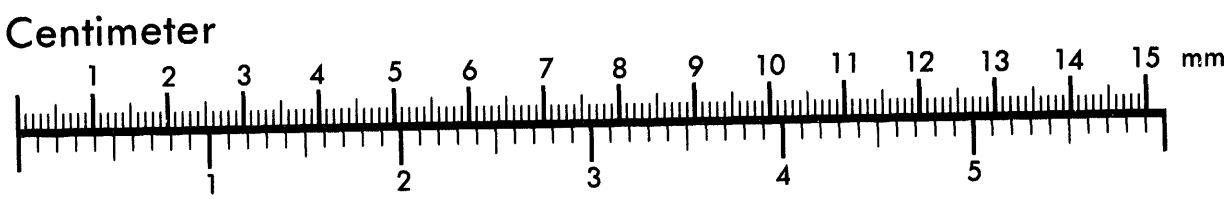

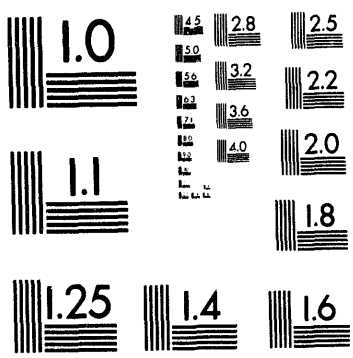

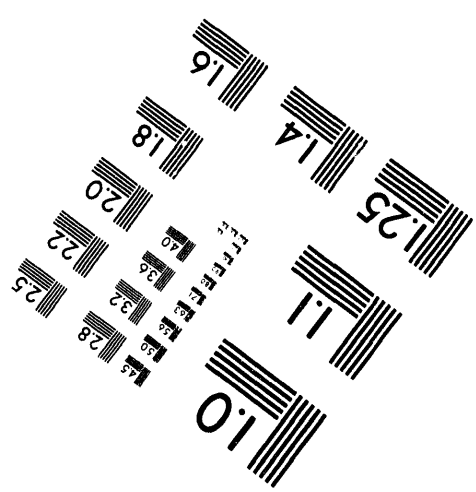

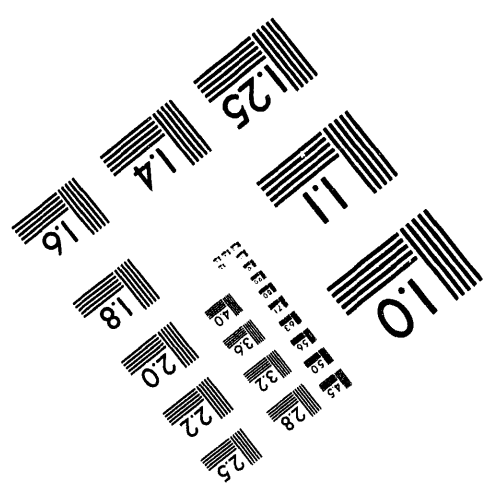

1 of 1

Conf-9406204--1

BNL-60437

Ferromagnetic Grain Boundary Signature in Die-Upset RE-Fe-B Magnets

L. Henderson Lewis, Yimei Zhu and D. O. Welch,

Materials Science Division, Department of Applied Science,

Brookhaven National Laboratory, Upton, N.Y. 11973

Abstract

Previous nanostructural and nanocompositional studies performed on the boundaries of deformed grains in two die-upset rare earth magnets with bulk compositions $Nd_{13.75}Fe_{80.25}B_6$ and $Pr_{13.75}Fe_{80.25}B_6$ indicate that the intergranular phase in many grain boundaries is enriched in iron relative to the bulk. We present here preliminary magnetic data that provide further evidence that this grain boundary phase is indeed iron-rich, and in fact appears to be ferromagnetic. Hysteresis loops were performed at 800 K on die-upset magnets with the above compositions. Each sample showed a clear hysteresis with coercivities between 34 and 40 Oe average remanence $4\pi M_R$ of 6.8 G for the Nd-based sample and 10.3 G for the Pr-based sample. The ferromagnetic signals measured at high temperature in these magnets are attributed to the iron-rich grain boundary phase. The implications of this conclusion with respect to coercivity are discussed.

Introduction:

Coercivities of magnets based on the 2-14-1 rare earth - iron - boron phase are typically in the range of 12 - 16 kOe, with reports ranging to over 24 kOe for a melt-spun then hot-pressed magnet with the complex composition $(Pr_{13.75}Fe_{0.95}Co_{0.05})_{80.25}B_6)_{0.996}Ga_{0.004}$ (1). However, the anisotropy field of

L.Henderson Lewis, Yimei Zhu and D. O. Welch: "Novel Magnetic Structures and Properties" - Acta Met. Meeting; Santa Fe, June 24-25, 1994

$Nd_2Fe_{14}B$ at room temperature is around 90 kOe (2), a value that is over four times larger than the typical magnet coercivities; clearly a lower-energy route for magnetic reversal is operative in these magnets. This relatively low value of coercivity contributes to energy products that are only roughly two-thirds of the theoretically possible energy products.

In order to engineer Fe-Nd-B magnets with improved energy products, it is necessary to identify the correct mechanism by which magnetic reversal occurs. There is a consensus within the literature that sintered magnets based on the 2-14-1 phase achieve their coercivity via the nucleation of reversed domains (3); however, the picture is not so clear-cut in the case of those magnets produced by melt-quenching and die-upsetting. Researchers from General Motors Corporation Research and Development Center believe that the coercivity in these magnets is determined by strong pinning of domain walls by a non-magnetic intergranular phase (4, 5). In contrast, studies that compare the hysteretic properties fit to theoretical models as well as calculated activation volumes of both sintered and melt-spun magnets have prompted some researchers (6-8) to conclude that the nucleation mechanism is dominant in both die-upset and sintered magnets. Recent data obtained from magnetic viscosity measurements (9) on melt-quenched magnets agree with this claim.

Nanostructural, nanocompositional and initial magnetization studies (10) were recently performed on two rare-earth magnets based on the 2-14-1 composition produced by melt quenching followed by die-upsetting. The results of these studies indicate that the dominant contribution to coercivity seems to be the nucleation of reversed domains. These reversed domains are hypothesized to originate in the lower-anisotropy, iron-rich regions that surround the grains of the main 2-14-1 phase. We present here further evidence of the existence of iron-rich grain boundaries in these magnets. Moreover, it appears that the grain

boundary phase is ferromagnetic, a result that has important implications for the magnetic coupling between the grains.

Experimental Procedures:

The hysteresis loops of two die-upset rare-earth magnets obtained from General Motors Research and Development Center were measured using a SQUID magnetometer manufactured by Quantum Design. The bulk compositions of the magnets are $Nd_{13.75}Fe_{80.25}B_6$ and $Pr_{13.75}Fe_{80.25}B_6$; they were fabricated by standard hot deformation processing methods (11) in which overquenched melt-spun ribbons were hot pressed at 750°C and then further deformed at 800°C to produce oriented die-upset magnets. Additional processing details are outlined in references 1 and 12.

Each sample was machined down to the appropriate dimensions to fit inside a quartz capillary tube of 2 mm (i.d.) x 3 mm (o.d.). The samples were cut using a stainless-steel wire saw and were subsequently polished with 600 grit silicon carbide paper; the final dimensions were 1.423 mm x 1.217 mm x 1.933 mm for the Nd-based sample and 1.264 mm x 1.255 mm x 2.008 mm for the Pr-based sample (measurements are estimated to be accurate to ±0.001 mm). Solid quartz rods of average 1.56 mm diameter were used on either side of the specimen for support within the capillary tube. Zirconium turnings were added as a getter and the tubes were evacuated to a base pressure of 5.6×10^{-5} torr then sealed to avoid the possibility of oxidation during measurement. Prior to each hysteresis loop measurement the magnets were brought to a temperature of 800 K and then saturated in an applied field of +55 kG. The resultant hysteresis loops were corrected for demagnetization using the equations (13):

$$H_{int} = H_{appl} - H_{demag} \qquad (1)$$

$$H_{demag} = 4\pi M_S \times (2/\pi) \times \arcsin(1/1+q) \qquad (2)$$

In the above expression M_S is the magnetization and q is the dimensional ratio; H_{demag} was further multiplied by a constant correction factor of 0.815 that was obtained from a measurement of very low coercivity nickel. The maximum standard deviation in the measurement of the sample moment is about 0.3%. In order to compute the magnetization in Gaussian units, the measured moment was divided by the total volume of the specimen.

Results:

The magnetic hysteresis loops obtained at T = 800 K, corrected as discussed above, are displayed in Figures 1a and 1b. Both hysteresis loops show cooperative ferromagnetic behavior that begins at an internal field of 300 G. The coercivity H_c, taken as half of the loop width, is 34 Oe for the Nd-based sample and is 40 Oe for the Pr-based sample. The remanent magnetization $4\pi M_R$, taken as half of the loop height, is 6.8 G for the Nd-based sample and is 10.3 G for the Pr-based sample. The origin of the asymmetry in the loops is unknown, although it could result from slight movement of the specimens within the quartz tube. The surface condition of the samples appeared to be unchanged from that prior to measurement, but a portion of the zirconium getter in the Pr-based sample acquired a goldish tint, indicative of ZrO_2 formation. The magnetization in either specimen does not saturate with increasing applied field, but rather continues to increase in a paramagnetic manner.

Discussion:

The following results are summarized from previous work (10, 14, 15) that characterized the die-upset magnet samples with high-resolution TEM and SQUID magnetometry performed at elevated temperatures: The microstructures of both the Nd-based and the Pr-based die-upset magnets are

very similar and are highly anisotropic, consisting mostly of platelet-shaped grains of the 2-14-1 phase stacked parallel to their *c*-axes and separated from one another by a thin intergranular phase in some, but not all, grain boundaries The interior of some of the grains contains a speckling of RE-rich precipitates, as shown in Figure 2; however, the more platelet-shaped grains with a higher aspect ratio than those shown in Figure 2 are largely free of such precipitates. The microstructure is also decorated with large pockets of $Nd_{70}Fe_{30}$ at triple junctions as well as rare-earth oxides that seem to congregate along the constituent ribbon boundaries (16). In many grain boundaries the intergranular phase is amorphous, iron-rich relative to the bulk grain composition, and its presence is dependent upon the relative orientation of the 2-14-1 platelets (10). The relative concentrations of boron were not examined. The average width of the intergranular phase is 8 - 12 Å in the Nd-based magnet and is 15 - 20 Å in the Pr-based magnet. The initial magnetization curves of both samples show a steep temperature-independent rise in the magnetization followed by an approach to saturation that is temperature-dependent; the same trend is also illustrated in the development of the coercivity with applied field. The magnetic results are characteristic of nucleation-controlled coercivity development (17).

The present work was motivated by a desire to investigate whether or not a magnetic signature of the grain boundary phase is detectable. We believe that the origin of the ferromagnetic signal obtained at 800K in these samples is the iron-rich grain boundary region. The signal is not from the main 2-14-1 phases themselves because the reported Curie temperatures are T_c = 565 K for $Pr_2Fe_{14}B$ and T_c = 585 K for $Nd_2Fe_{14}B$ (18). The reversible rise of the hysteresis loop with applied field for $H_{appl} > 300$ G or $H_{appl} < -300$ G probably originates from the paramagnetic response of the main 2-14-1 phases above their respective Curie temperatures.

Other phases present in the die-upset magnets, either reported or hypothesized, might be magnetic but it is unlikely that most of these phases would contribute to the ferromagnetic signal found at 800 K. Crystalline FeB has a Curie temperature of 598 K (19), while the amorphous iron-borides all have Curie temperatures in the range of 500 K to 600 K (20). It is possible, however, that a form of Fe_2B (T_c = 1013 K (21)) is represented within the grain boundary phase. Rare-earth - iron intermetallic phases such as Nd_2Fe_{17} and Pr_2Fe_{17} have Curie temperatures near room temperature (22), and disordered forms of these compounds would be expected to have yet lower Curie temperatures.

The presence of ferrimagnetic iron oxides, in the form of either γ-Fe_2O_3 (T_c = 948 K) or Fe_3O_4 (T_c = 858 K) (23), would indeed provide a ferromagnetic contribution to the hysteresis loop at high temperatures; traces of these iron oxides could have been formed in any of the many processing steps that occur before the final die-upset magnet is formed. However, the standard enthalpy of formation (ΔH°_{298}) of the rare-earth oxides, which are not ferromagnetic, is much larger than that of analogous iron oxides. For example, the standard enthalpy of formation of α-Fe_2O_3, the most stable form of iron oxide, is -196.3 kcal/mol, while that of Pr_2O_3 is -436.8 kcal/mol and Nd_2O_3 is -432.1 kcal/mol (24). This thermodynamic principle, combined with the fact that the magnets' starting compositions are approximately 20% richer in the rare earth component than the stoichiometric composition, renders the formation of magnetic iron oxides an unlikely event.

Other factors implicate the grain boundary phase as the source of the ferromagnetic hysteresis loop. The remanence of the Pr-based sample is larger than that of the Nd-based sample, a difference which is reflected in the larger thickness of grain boundary phase measured for the Pr-based sample. It is

doubtful that the signal originates from a surface contamination, because the larger signal derives from the sample with the smaller surface area.

Conclusions:

We present here further evidence that the intergranular phase in die-upset magnets with bulk compositions $Nd_{13.75}Fe_{80.25}B_6$ and $Pr_{13.75}Fe_{80.25}B_6$ is iron-rich, and additionally appears to be ferromagnetic. These two conclusions have important ramifications with regards to the engineering of melt-quenched magnets with optimal properties based on the 2-14-1 composition. The existence of ferromagnetic grain boundaries would promote strong exchange coupling between the grains themselves, and thus cause the grains to act cooperatively during magnetic reversal. Recent micromagnetic calculations (25) of nucleation fields of 2-D magnetic structures conclude that grains with direct exchange interactions can easily cause catastrophic demagnetization of the entire sample after the reversal of one grain. Additionally, the presence of a ferromagnetic intergranular phase allows for the existence of lower-anisotropy sites for reverse domain nucleation while at the same time it reduces the probably of domain wall pinning to occur at the intergranular phase.

An ideal microstructure for a nucleation-type magnet consists of grains of a magnetically hard phase that are exchange-isolated from one another (26), ideally by a thin coating of a non-magnetic phase. Therefore, segregation of non-magnetic atoms to the ferromagnetic grain-boundary phase via metallurgical manipulation might serve to disrupt the intergranular exchange coupling and therefore would be expected to produce higher-coercivity, and thus higher energy product, magnets.

Acknowledgments:

We are grateful to C. D. Fuerst for providing us with samples and for helpful discussions. This research was sponsored by US DOE Laboratory Directed Research and Development Program, contract No. DE-AC02-76CH00016.

References:

1. C. D. Fuerst, E. G. Brewer, R. K. Mishra, Y. Zhu and D.O. Welch: *J. Appl. Phys.* **75** 4208 (1994)
2. K. H. J. Buschow: *Mat. Sci. Rep.* **1** (1) 1 (1986)
3. J. F. Herbst and J. J. Croat: *J. Magn. Magn. Mater.* **100** 57 (1991)
4. F. E. Pinkerton and C. D. Fuerst: *J. Appl. Phys.* **69** (8) 5817 (1991)
5. F. E. Pinkerton and C. D. Fuerst: *J. Magn. Magn. Mater.* **89** 139 (1990)]
6. M. Grönefeld and H. Kronmüller: *J. Magn. Magn. Mater.* **88** L267 (1990)
7. K.-D. Durst and H. Kronmüller: *J. Magn. Magn. Mater.* **68** 63 (1987)
8. D. Givord, Q. Lu, M. F. Rossignol, P. Tenaud and T. Viadieu: *J. Magn. Magn. Mater.* **83** 183 (1990)
9. L. Folks, R. Street, and R. Woodward: *J. Appl. Phys.* **75** (10) 6271 (1994)
10. L. Henderson Lewis, Y. Zhu and D. O. Welch: to be presented at the 6th Joint MMM-Intermag Conference, June 20 -23 1994, Abstract No. CB-02
11. R. W. Lee: *Appl. Phys. Lett.* **46** 790 (1985)
12. C. D. Fuerst and E. G. Brewer, *J. Appl. Phys.* **73** 5751 (1993)
13. D. J. Craik: Structure and Properties of Magnetic Materials pg 23, pub. by Pion Ltd., London (1971)
14. T.-Y. Chu, L. Rabenberg, R. K. Mishra: *J. Appl. Phys.* **69** (8) 6046 (1991)
15. R. K. Mishra, T.-Y. Chu, L. Rabenberg: *J. Magn. Magn. Mater.* **84** 88 (1990)
16. R. K. Mishra: *J. Appl. Phys.* **62** (3) 967 1987
17. G. C. Hadjipanayis and A. Kim: *J. Appl. Phys.* **63** (8) 3310 (1988)
18. J. F. Herbst: *Rev. Mod. Phys.* **63** (4) 819 (1991)
19. O. Beckman and L. Lundgren: Handbook of Magnetic Materials, Vol. 6, pg. 187; K. H. J. Bushow, Ed., North-Holland, 1991
20. K. Moorjani and J. M. D. Coey: Magnetic Glasses; Elsevier, 1984

21. O. Beckman and L. Lundgren: Handbook of Magnetic Materials, Vol. 6, pg. 216; K. H. J. Bushow, Ed., North-Holland, 1991

22. J. M. D. Coey: Proc. Inter. School Phys., Course CVI, pg. 265; G. F. Chiarotti, F. Fumi and M. P. Tosi, eds. North-Holland, 1990

23. S. Chikazumi and S. H. Charap: Physics of Magnetism, pg. 100; Robert E. Krieger Pub. Co, 1984

24. O. Kubaschewski, E. LL. Evans and C. B. Alcock: Metallurgical Thermochemistry; Pergamon Press 1967

25. T. Schrefl, H.F. Schmidts, J. Fidler, H. Kronmüller: *IEEE Trans. Magn.* **29** (6) 2878 (1993)

26. R. Ramesh and G. Thomas: *Mater. Sci. Eng.* **B3** 435 (1989)

Figure Captions:

Figure 1a: Hysteresis loop measured at 800 K for die-upset $Nd_{13.75}Fe_{80.25}B_6$

Figure 1b: Hysteresis loop measured at 800 K for die-upset $Pr_{13.75}Fe_{80.25}B_6$

Figure 2: Transmission electron micrograph illustrating Nd-rich precipitates within equiaxed grains of the $Nd_{13.75}Fe_{80.25}B_6$ magnet. The white scale marker represents 100 nm.

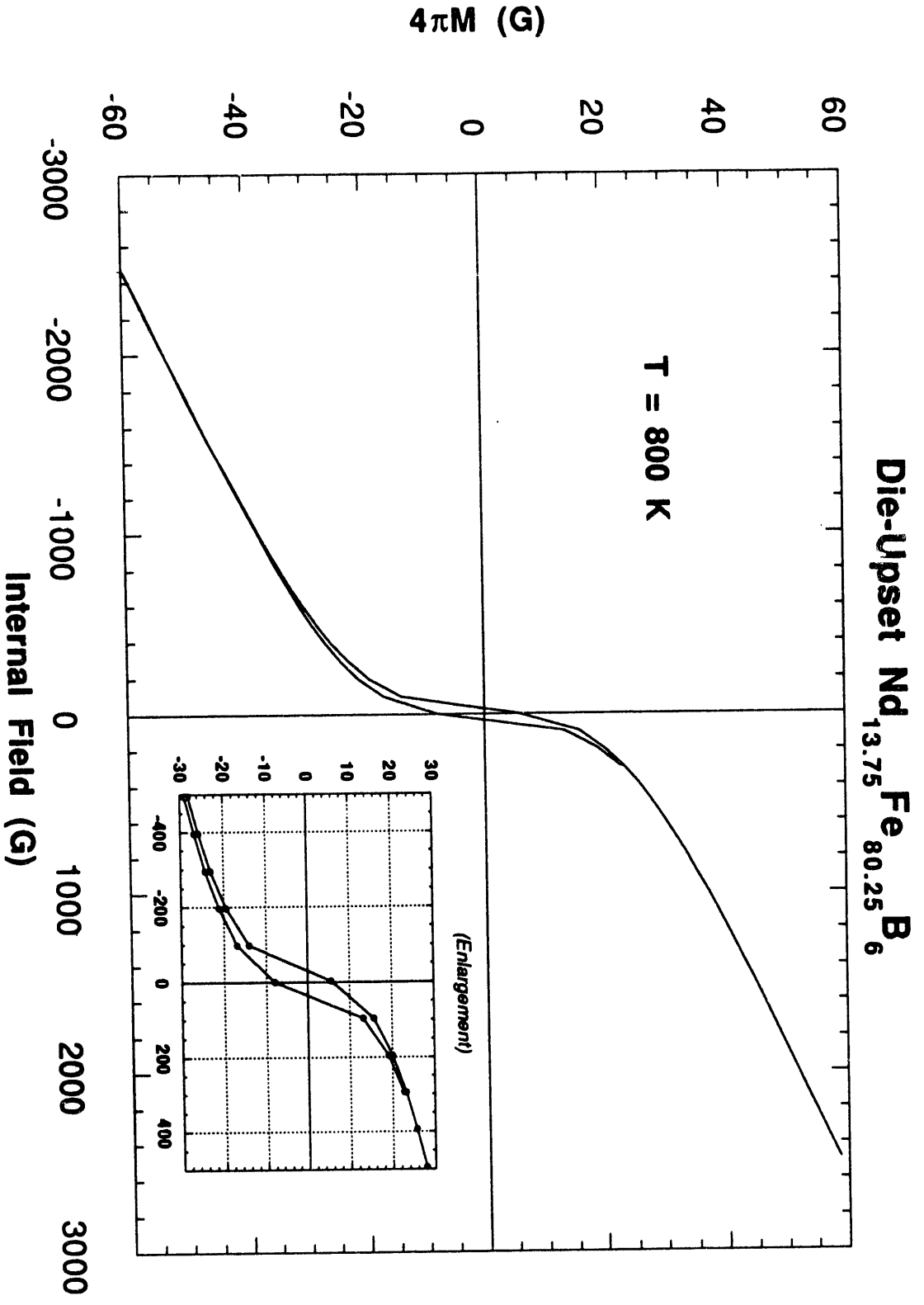
4πM (G)
60
40
20
0
-20
-40
-60
Die-Upset $Nd_{13.75}Fe_{80.25}B_6$
T = 800 K
(Enlargement)
30
20
10
0
-10
-20
-30
400
200
0
-200
-400
Internal Field (G)
3000
2000
1000
0
-1000
-2000
-3000

 Figure 1a

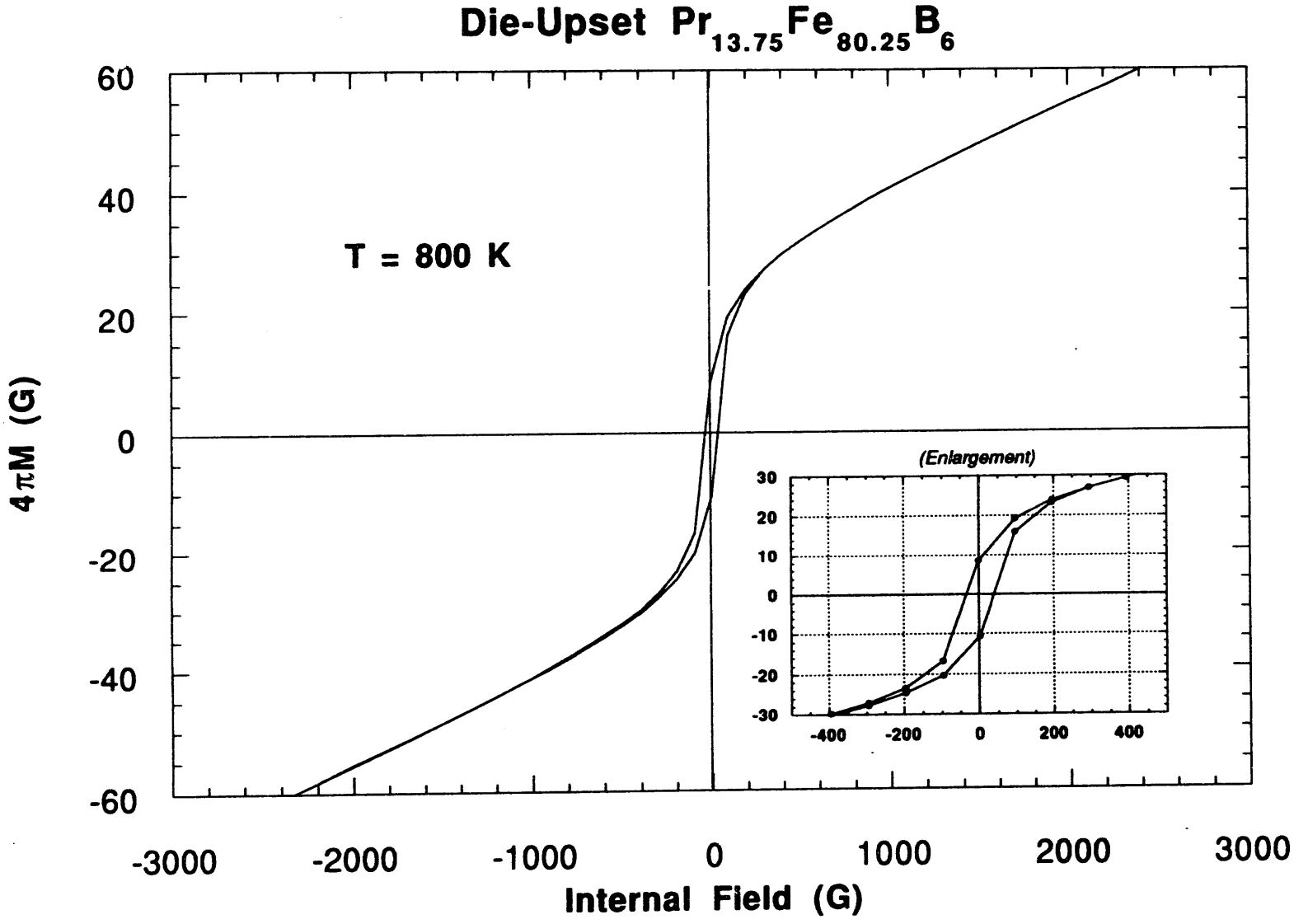

pg. 13 Figure 1b

pg. 14 Figure 2

DATE
FILMED
8/30/94
END